Efficient fourth harmonic generation of Nd:YAG laser in DKDP crystals.

G.Kruglik, N.Kondratyuk, A.Shagov

In Laser Optics 2001: Nonlinear Optical Phenomena and NonlinearDynamics of Optical Systems,
K.N.Drabovich, N.S.Kazak, V.A.Makarov, A.P.Voitovich, Editors,
Proceedings of SPIE vol.47518(SPIE, Bellingham,WA,2002) p.137

ABSTRACT

In the present work we investigated the conditions of the 4^{th} harmonic stable high effective pulse generation with the energy up to 100 mJ, efficiency ~ 50% and pulse repetition rate 10 Hz in DKDP crystals with noncritical phasematching. On the basis of experimental data we carried out the numerical modeling of thermal self-action effects influencing on the efficiency of the 4^{th} harmonic single-shot pulse generation and received the solution of non-stationary heat conduction equation, describing radial temperature profile in crystal as a function of time. It was shown that maximum efficiency of the 4^{th} harmonic generation in the thermal self-actions conditions is reached when initial crystal temperature is less than noncritical phasematching temperature and in the process of heating during the pulse inside the crystal radial temperature profile close to the noncritical phasematching temperature.

2. EXPERIMENT

At a present time the developing of high effective stable 4^{th} harmonic generators for pulsed Q-switched Nd:YAG lasers is still being actual. In the row of nonlinear crystals used for the 4^{th} harmonic generation DKDP crystals have a special place. In this crystals at low temperatures <100°C noncritical phasematching (NCPM) is realized and the efficiency of single-shot pulse generation is up to 75%.[1] However DKDP crystals absorb the 4^{th} harmonic radiation and have small temperature bandwidth.[1]Therefore the efficiency of the 4^{th} harmonic generation strongly depends on the effects of thermal self-actions due to inhomogeneous crystal heating at radiation absorption at 266.[2]

In our experiments we used a commercial pulsed Q-switched Nd:YAG laser with the 2^{nd} harmonic generator (model LQ-727, Solar Laser System). This system provided 180 mJ, ~5 ns pulses at 532 nm. Pulse repetition rate varied from 0,9 Hz to 10 Hz. The divergence of the 2^{nd} harmonic pump beam ~ 5,7 mm in diameter was equal to ~ 0,7 mrad. The distribution of intensity in the cross-section was homogeneous and close to the rectangle profile. The measurements were carried out with two different ~ 93÷94% deuteration $12\times12\times20$ mm^3 DKDP crystals. DKDP crystals were installed inside copper heater, which temperature was regulated in the range 40°C-80°C and kept constant with accuracy ~ 0,1°C.

We revealed that during the low intensive 4^{th} harmonic radiation inside the DKDP crystals stable color-centers absorbing radiation at 266 nm are formed.[3] Fig.1 presents spectrum of DKDP crystals transmission before and after excitation at 266nm (~ 1 hour with $50MW/cm^2$).. In the sample №1 transmission decreased from T_{01}=91% (α_{01}=0,005cm^{-1}) to T_1=83% (α_1=0,05cm^{-1}), and in the sample №2 - from T_{02}=84% (α_{02}=0,045cm^{-1}) to T_2=52,5% (α_2=0,28cm^{-1}). UV-induced color-centers are stable to the temperature changing in the range 70…100°C and they remain stable during the prolonged time (>72 hours).

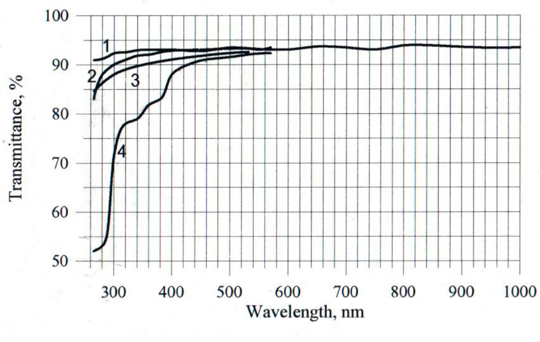

Fig.1. Absorption spectrums of DKDP crystals before (1,3) and after (2,4) excitation at 266 nm:
1,2 – for sample №1, 3,4 – for sample №2.

For both samples we measured the dependencies of the 4^{th} harmonic efficiency $\eta_{4\omega}$ versus the 2^{nd} harmonic intensity $I_{2\omega}$ at pulse repetition rate f=0,9Hz, when connected with heat accumulating effects due to the 4^{th} harmonic absorption are insignificant (fig.2). It is seen that at pulse intensities $I_{2\omega} > 60MW/cm^2$ efficiencies $\eta_{4\omega}$ saturate at the level ~ 52 % and ~ 40% in samples №1 and №2 respectively.

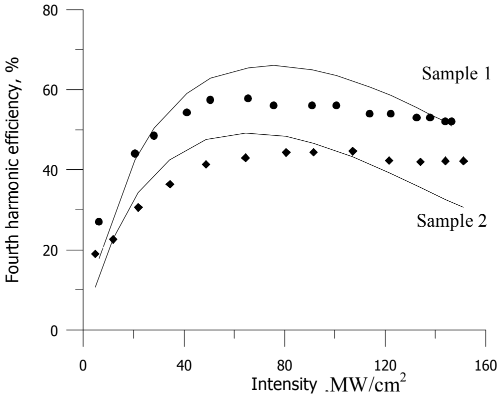

Fig.2 Fourth harmonic conversion efficiency v.s. second harmonic intensity. The symbols depict the experimental data and the solid curves show the best numerical fit.

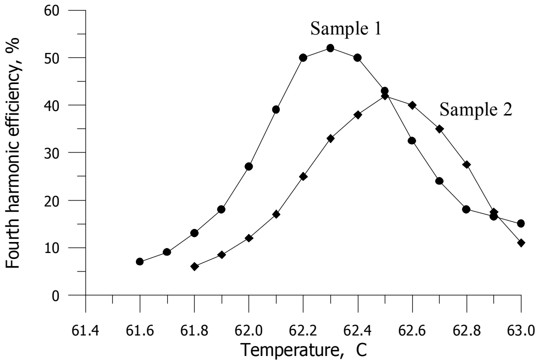

Fig.3. Fourth harmonic efficiency as a function of temperature in a 2-cm –long DKDP crystals at intensity $I_{2\omega} \approx 100$ MW/cm^2

We measured the phasematching temperature curves for both samples at the intensity $I_{2\omega} \approx 100MW/cm^2$ and pulse repetition rate f=0,9 Hz (fig. 3). At temperatures t_{1pm}=62,3°C and t_{2pm}=62,5°C in samples №1 and №2 respectively NCPM was realized.

For a stable 4^{th} harmonic pulses receiving with the pulse repetition rate f=10 Hz initial thermostat temperature was installed lower than NCPM temperature. At initial thermostat temperatures t_{01}=61,7°C and t_{02}=61,9°C for samples №1 and №2 respectively the stable 4^{th} harmonic pulses with the energy $E_{4\omega}^{(1)}$=66mJ and $E_{4\omega}^{(2)}$=51mJ and the efficiency $\eta_{4\omega}^{(1)}$=52% and $\eta_{4\omega}^{(2)}$=40% respectively were obtained. In this case the pump beam diameter of the 2^{nd} and the 4^{th} harmonic was equal to 5.7 мм. Stable conditions of the 4^{th} harmonic pulse generation with the energy $E_{4\omega}^{(1)}$=90mJ and the efficiency $\eta_{4\omega}^{(1)}$=53% was obtained in sample №1 at increasing the pump beam diameter up to 7 mm. At the expense of additional crystal heating with the 4^{th} harmonic radiation within several minutes stable conditions of the 4^{th} harmonic generation without mechanic angle tuning was provided (fig.4).

$E_{4\omega}$=90mJ, $I_{4\omega}$=45 MW/cm^2, $\eta_{4\omega}$=52%.

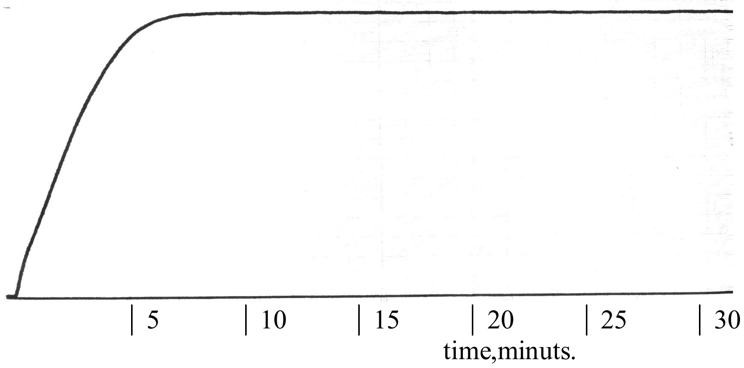

Fig.4. Long term stability of fourth harmonic in DKDP crystal at 90°-temperature noncritical phase matching: for 532 nm with f=10 Hz, $E_{2\omega}$=170mJ, τ=5ns, ∅=7mm, $I_{2\omega}$=88MW/cm^2.

Thus we made the conclusion that for a stable high effective 4th harmonic generation is necessary that

- before the beginning of the pulse generation initial crystal temperature must be less than NCPM temperature and must be in the limits of temperature phasematching curve,
- temperature variation range of the crystal at the time of the 4th harmonic pulse generation must be in the limits of temperature phasematching curve and
- separating heat must be transmitted to the thermostat during the time less than pulse sequence period.

3. NUMERICAL MODELING OF THE 4TH HARMONIC SINGLE SHOT PULSE GENERATION

In this case there is temperature mismatch [2]:

$\Delta k = \frac{4\pi}{\lambda_{2\omega}} \cdot \left.\frac{\partial B}{\partial T}\right|_{T=T_{pm}} \cdot (T - T_{pm})$, where $\frac{\partial B}{\partial T} = \frac{0{,}886 \cdot \lambda_{2\omega}}{4 \cdot \ell \cdot \Delta T_{pm}}$ is dispersive birefringence, ΔT_{pm} - temperature bandwidth, ℓ - crystal length. In quasi-static approximation the pulse was approximated with the step-wise function with the step width Δt and fixed amplitude for each step. For step number n heat balance equation at point (z) has the form

$$c \cdot \rho \cdot (T_n - T_{n-1}) = \left[\alpha_{2\omega} \cdot I_{2\omega}(z, t_n) + \alpha_{4\omega} \cdot I_{4\omega}(z, t_n)\right] \cdot \Delta t,$$

where c is specific heat, ρ - crystal density, $\alpha_{2\omega}$ and $\alpha_{4\omega}$ - linear absorption coefficients, $I_{2\omega}$ and $I_{4\omega}$ - harmonic intensities, T_{n-1} - crystal temperature for previous step number n-1, T_n - crystal temperature for step number n after the heating. Then temperature change during the time $n \cdot \Delta t$

$$\Delta T_n(z) = \frac{1}{c\rho} \sum_{m=1}^{n} \left[\alpha_{2\omega} \cdot I_{2\omega}(z, t_n) + \alpha_{4\omega} \cdot I_{4\omega}(z, t_n)\right] \cdot \Delta t.$$

The initial system of equations governing the fields E_2 and E_4 during nonlinear frequency conversion in DKDP from $\omega_2 = 2\omega$ to $\omega_4 = 4\omega$ is [2]

$$\begin{cases} \frac{dE_2(z,t)}{dz} = -\frac{\omega_2 \cdot d_{eff}}{n \cdot c_o} \cdot E_2 \cdot E_4 \cdot \sin\theta - \frac{1}{2} \cdot \alpha_{2\omega} \cdot E_2, \\ \frac{dE_4(z,t)}{dz} = 2 \cdot \frac{\omega_2 \cdot d_{eff}}{n \cdot c_o} \cdot E_2^2 \cdot \sin\theta - \frac{1}{2} \cdot \alpha_{4\omega} \cdot E_4, \\ \frac{d\theta}{dz} = \Delta k - \frac{2\omega_2 \cdot d_{eff}}{n \cdot c_o} \cdot \left(E_4 - \frac{E_2^2}{E_4}\right) \cdot \cos\theta, \end{cases}$$

where d_{eff} is effective nonlinear coefficient, n – refractive index, c_o – speed of light in vacuum.

Fig.2 presents calculated 2w-to-4w frequency conversion efficiency curves for two DKDP crystals. In both cases there is a good correlation between experimental results and calculated dependencies. By means of numerical modeling we determined the value of temperature gradient along z axis , (fig.5). It is seen that maximal conversion efficiency is reached when temperature gradient along z axis varies according to the linear law and exists within phasematching temperature curve.

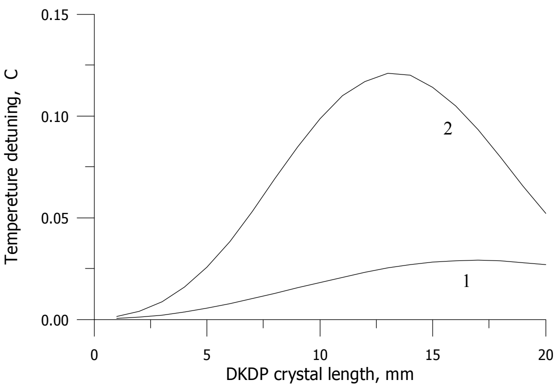

Fig.5. Calculated profile of temperature detuning along z-axis in DKDP crystal 1 – for maximal efficiency $\eta_{4\omega}$ = 66% at $E_{2\omega}$=97mJ and $I_{2\omega}$=76 MW/cm^2, 2 – for saturation efficiency $\eta_{4\omega}$ = 51% at $E_{2\omega}$=187mJ and $I_{2\omega}$=146 MW/cm^2.

3. TRANSIENT HEAT PROPAGATION PROCESSES AT THE 4TH HARMONIC GENERATION MODELING

For simplifications we made the following assumptions: DKDP absorption and its heat conductivity are isotropic, there is homogeneous radial heating, beam diameter of the 4th harmonic is significantly smaller than crystal size, separating heat has no influence on the thermostat temperature, heat exchange comes about crystal lateral surface, crystal end-walls are heat-insulated, separated during the pulse generation hear is instantaneous.

Then initial temperature conditions taking into consideration arbitrary starting temperature choice have the form:

$$U(x,y,z,0)=\begin{cases}U_0(z), & \text{if } x^2+y^2<R^2\\ 0, & \text{if } x^2+y^2>R^2\end{cases},$$

where x and y – coordinates of a considered point situated inside the 4th harmonic beam with radius R. Let U(x,y,z,t)=T(x,y,z,t)-U_c, where U_c is initial thermostat and crystal temperature before the 4th harmonic pulse generation.

In the absence of boundary conditions in (x,y) plane the heat conduction equation for the three dimensional case can be written as:

$$\frac{\partial U}{\partial t}=a^2\left(\frac{\partial^2 U}{\partial x^2}+\frac{\partial^2 U}{\partial y^2}+\frac{\partial^2 U}{\partial z^2}\right), \tag{1}$$

where $a^2=\dfrac{k}{c\cdot\rho}$ - temperature conduction coefficient, k – heat conduction coefficient, c – specific heat, ρ - crystal density.

Particular solution of eq. (1) has the form:

$$U(x,y,z,t)=C_{(k_x+k_y)}\cdot C_{k_z}\cdot e^{i(k_x\cdot x+k_y\cdot y+k_z\cdot z)-a^2\cdot k^2\cdot t} \tag{2}$$

where $k^2=k_x{}^2+k_y{}^2+k_z{}^2$.

Parameters k_x and k_y in the absence of boundary conditions in (x,y) plane can take up any value from -∞ to +∞.

Along z-axis there are boundary conditions

$$\left.\frac{\partial U}{\partial z}\right|_{z=0}=0 \quad\text{and}\quad \left.\frac{\partial U}{\partial z}\right|_{z=L}=0, \tag{3}$$

and parameter k_z takes up discrete values $k_z^{(n)}=\dfrac{\pi\cdot n}{L}$, n =0; ± 1; ± 2 …

In this case equal1 solution can be represent as superposition of particular solution having the form

$$U(x,y,z,t)=\int_{-\infty}^{+\infty}dk_x\int_{-\infty}^{+\infty}dk_y C(k_x,k_y)e^{i(k_x\cdot x+k_y\cdot y)}\cdot\sum_{n=-\infty}^{+\infty}C_n e^{i\cdot k_z^{(n)}z-a^2k^2t}, \tag{4}$$

which after transformations and taking into consideration boundary and initially conditions has the form:

$$U(x,y,z,t)=\frac{1}{4\pi a^2 t}\int_0^L dz'\int_{-\infty}^{+\infty}dx'\int_{-\infty}^{+\infty}dy' U(x',y',z',0)\cdot\exp\left[-\frac{(x-x')^2+(y-y')^2}{4a^2t}\right]\cdot$$

$$\cdot\sum_{n=-\infty}^{+\infty}\cos\left(\frac{\pi n}{L}\cdot z\right)\cdot\cos\left(\frac{\pi n}{L}\cdot z'\right)\cdot e^{-a^2\cdot\left(\frac{\pi n}{L}\right)^2\cdot t}. \tag{5}$$

If for t=0 the temperature along z-axis varies according the linear law

$$U(x,y,z,0)=\alpha\cdot z, \tag{6}$$

where α is proportion coefficient, then for the chosen cut with z coordinate where $x_1<x<x_2$ and $y_1<y<y_2$ expression (5) can be represented in the form:

$$U(x,y,z,t)=\frac{1}{4}\cdot\left[\Phi\left(\frac{x-x_1}{2a\sqrt{t}}\right)-\Phi\left(\frac{x-x_2}{2a\sqrt{t}}\right)\right]\cdot\left[\Phi\left(\frac{y-y_1}{2a\sqrt{t}}\right)-\Phi\left(\frac{y-y_2}{2a\sqrt{t}}\right)\right]\cdot\frac{\alpha\cdot L}{2}\cdot A_{n,t}, \qquad (7)$$

where $\Phi\left(\frac{x-x_1}{2a\sqrt{t}}\right)$, $\Phi\left(\frac{x-x_2}{2a\sqrt{t}}\right)$, $\Phi\left(\frac{y-y_1}{2a\sqrt{t}}\right)$ and $\Phi\left(\frac{y-y_2}{2a\sqrt{t}}\right)$ - probability integrals (error functions):

$$\Phi(\xi)=\frac{2}{\sqrt{\pi}}\int_0^{\xi}e^{-\mu^2}d\mu \quad \text{and} \quad A_{n,t}=\left[1-\frac{8}{\pi^2}\sum_{n=1}^{\infty}\frac{1}{(2n-1)^2}\cos\left(\frac{\pi}{L}(2n-1)z\right)\cdot e^{-a^2\left(\frac{\pi}{L}(2n-1)^2 t\right)}\right].$$

It is easy to make sure that when $t\to 0$ for z=L:

$$U(x,y,z,0)=\frac{1}{4}\cdot[\Phi(\infty)-\Phi(-\infty)]\cdot[\Phi(\infty)-\Phi(-\infty)]\cdot\frac{\alpha\cdot L}{2}\cdot 2=\alpha\cdot L, \qquad (8)$$

that corresponds the initial conditions (6). In the factor $A_{n,t}$ we restrict only with the first term of the sum because of smallness of following terms:

$$A_{n,t}=1+\frac{8}{\pi^2}\cdot e^{-\left(\frac{a\cdot\pi}{L}\right)^2\cdot t} \qquad (9$$

For the temperature radial profile calculations in the crystal output in the cut z=L in different periods of time let embed normalized temperature function of the form

$$f(x,y,L,t)=\frac{U(x,y,L,t)}{U(x,y,L,0)}=$$

$$=\frac{1}{8}\left[\Phi\left(\frac{x-x_1}{2a\sqrt{t}}\right)-\Phi\left(\frac{x-x_2}{2a\sqrt{t}}\right)\right]\cdot\left[\Phi\left(\frac{y-y_1}{2a\sqrt{t}}\right)-\Phi\left(\frac{y-y_2}{2a\sqrt{t}}\right)\right]\cdot\left[1+\frac{8}{\pi^2}\cdot e^{-\left(\frac{a\cdot\pi}{L}\right)^2\cdot t}\right] \qquad (10)$$

Fig. 6 represents calculated values of normalized temperature function at the output face in 2-cm long DKDP crystal with beam radius R=3 mm in different periods of time 0,01s; 0,1s; 1s and 10s.

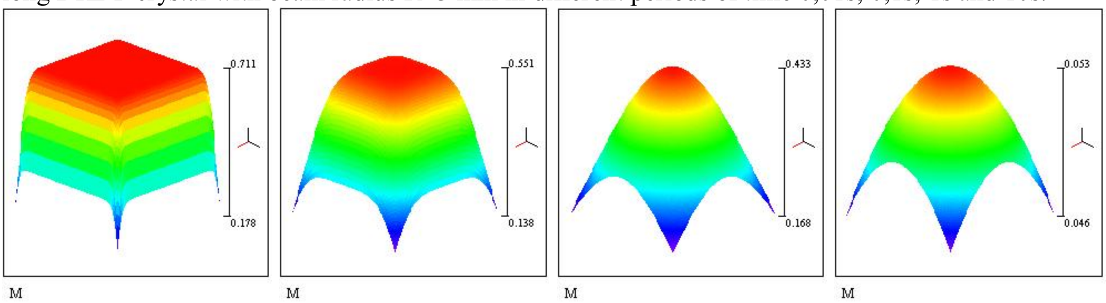

t=0,01s t=0,1s t=1s t=10s

Fig.6 Three-dimensional illustrations of the radial temperature profile at the output face of DKDP crystal

In the process of heat exchange inside the crystal there is inhomogeneous temperature profile with the maximum on the 4th harmonic beam axis. If pulse repetition rate is less than heat exchange process duration the following proceses of 4th harmonic generation occurs in the conditions when temperature mismatch exists and wave mismatch is maximal on the beam axis. It is obvious that there are conditions when during the next pulse generation inside the crystal homogeneous temperature profile close to the NCPM temperature restores when the efficiency of the 4th harmonic generation is maximal.

With the purpose of this conditions determination we found from (5) the expressions describing temperature fields on the axis (r=0) and lateral surface (r=R) of cylinder in the cross z=L/2:

$$\text{for } r=0 \quad U_1(x,y,\frac{L}{2},t) = \left(1 - e^{-\frac{R^2}{4a^2 t}}\right)\frac{\alpha L}{2}, \qquad (11)$$

$$\text{for } r=R \quad U_2(x,y,\frac{L}{2},t) = \left(1 - e^{-\frac{R^2}{2a^2 t}} \cdot I_0\left(\frac{R^2}{2a^2 t}\right)\right)\frac{\alpha L}{2}, \qquad (12)$$

which at $t \to 0$ satisfy the conditions (6).
Let us assume that in the point of time t immediate heat pulse which restores homogeneous temperature profile operates the crystal. Then on the cylinder axis

$$U_1(0,\frac{L}{2},t) + \delta T_1(0,\frac{L}{2}) = \frac{\alpha L}{2} \qquad (13)$$

and on the lateral surface

$$U_2(R,\frac{L}{2},t) + \delta T_2(R,\frac{L}{2}) = \frac{\alpha L}{2}. \qquad (14)$$

In this case heat pulses values $\delta T_1(0,\frac{L}{2}) = \frac{\alpha \cdot L}{2} \cdot e^{-\frac{R^2}{4a^2 t}}$ and.

$$\delta T_2(R,\frac{L}{2}) = \frac{\alpha \cdot L}{2} \cdot e^{-\frac{R^2}{2a^2 t}} \cdot I_0\left(\frac{R^2}{2a^2 t}\right)$$

For the temperature radial profile calculations in the crystal in the cut z=L/2 in different periods of time let embed normalized heat pulses function of the form

$$\gamma = \frac{\delta T_2(R, L/2)}{\delta T_1(0, L/2)} = e^{-\frac{R^2}{2a^2 t}} \cdot I_0\left(\frac{R^2}{2a^2 t}\right) \qquad (15)$$

As heat generation capacity depends on the 4th harmonic intensity, than relation (15) characterizes the depth of the intensity profile in the central path of beam and time t is the period of pulse sequence of the 4th harmonic. From (15) in follows that at $t \to \infty$ $\gamma \to 1$. This means that in single-shot pulse beam radial profile of the 4th harmonic intensity $I_{4\omega}$ is homogeneous and the efficiency $\eta_{4\omega}$ is maximal.

In fig.7 we represented calculated dependencies $\gamma(t)$ for the beams of the 4th harmonic with different radius R 1,5mm, 2,0mm и 3,0 mm. It is seen that with time t decreasing (which is similar to the repetition rate increasing) depth of the intensity profile in the central path of beam increases and consequently the efficiency of the 4th harmonic generation decreases. From the other side with the constant repetition rate the depth of the intensity profile in the narrow beams is smaller than in the wide ones. This leads to the conclusion that at the same pulse repetition rate the efficiency $\eta_{4\omega}$ in narrow beams is higher than in wide ones.

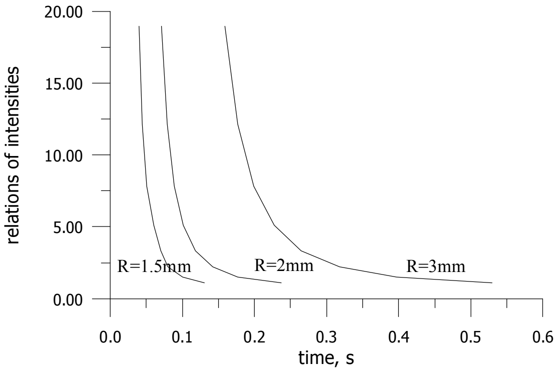

Fig.7. Calculated time-dependent relations of intensities in edge to center of fourth harmonic beam. In this case the homogeneously radial temperature profile in DKDP crystal will be generated after fourth pulse actions.

For confirmation of the obtained results and our conclusions we investigated experimentally the efficiency of the 4th harmonic generation of Nd:YAG laser in 2cm-long DKDP crystal depending on the pulse repetition rate and beam diameter. This system operated at 532 nm and generated pulses with the energy $E_{2\omega}$=370mJ and pulsewidth τ=10ns. The 4th harmonic 7 mm diameter pump beam had a divergence ~ 1 mrad. The dependence $\eta_{4\omega}$ versus the pulse repetition rate is given in fig.8. It is clear that when repetition rate increases the efficiency $\eta_{4\omega}$ decreases. At the pulse repetition rate f=10Hz the efficiency $\eta_{4\omega}$ was very small and in the 4th harmonic radial profile of the intensity was strongly inhomogeneous with the typical failure in the center of the beam. However when using aperture diaphragms with diameters 2,6 mm, 4 mm, 5 mm, 5,5 mm we managed to obtain stable 4th harmonic generation with the efficiency up to 50%.

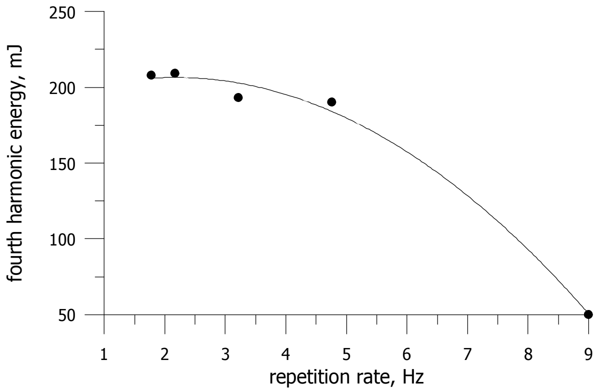

Fig.8. Fourth harmonic energy v.s. repetition rate of pulses:$E_{2\omega}$=370mJ, τ=10 ns, ∅=7mm, $I_{2\omega}$=96MW/cm^2.

4. CONCLUSION

On the basis of obtained data we developed the 4th harmonic generator of Nd;YAG laser model LG-104, produced by the company Solar LS. The 4th harmonic generator LG-104 provides the opportunity to obtain a stable pulse with the energy up to 100 mJ, efficiency ~ 50% at pulse repetition rate 10 Hz. At that the time of stable 4th harmonic generation establishing is less than 10 min.

5. REFERENCES

1. Handbook of nonlinear optical crystals/ V.G.Dmitriev, G.G.Gurzadyan, D.N.Nikogosyan (Berlin, Springer-Verlag, 1997).
2. Applied nonlinear optics/ V.G.Dmitriev, L.V.Tarasov (Moskow, Radio and connection,1982).
3. C.D.Marshall, S.A.Payne, M.A.Henesian, S.A.Speth, H.T.Powell. J.Opt.Soc.Am. B., 11, 774 (1994).